Spectrochimica Acta Part A 74 (2009) 1016–1024

Contents lists available at ScienceDirect

Spectrochimica Acta Part A: Molecular and Biomolecular Spectroscopy

journal homepage: www.elsevier.com/locate/saa

Ligating behaviour of Schiff base ligands derived from heterocyclic β-diketone and ethanol or propanol amine with oxovanadium (IV) metal ion

B.T. Thaker*, R.S. Barvalia

Department of Chemistry, Veer Narmad South Gujarat University, Surat 395007, Gujarat, India

ARTICLE INFO

Article history:
Received 2 January 2009
Accepted 19 August 2009

Keywords:
Oxovanadium (IV) complexes
FT-IR
ESR spectrometry
Thermal studies

ABSTRACT

Synthesis and evaluation of six new oxovanadium (IV) complexes, formed by the interaction of vanadyl sulphate pentahydrate and the Schiff base, viz.; (HL^1)–(HL^3) and (HL^4)–(HL^6) such as 5-hydroxy-3-methyl-1(2-chloro)phenyl-1H-pyrazolone-4-carbaldehyde (I), 5-hydroxy-3-methyl-1(3-chloro)phenyl-1H-pyrazolone-4-carbaldehyde (II) and 5-hydroxy-3-methyl-1(3-sulphoamido)phenyl-1H-pyrazolone-4-carbaldehyde (III) with ethanol amine and propanol amine, respectively, in aqueous ethanol medium. The ligands and their Schiff base ligands have been characterized by elemental analyses, IR and ^{1}H NMR. The resulting complexes have been characterized by elemental analyses, IR, ^{1}H NMR, mass, electronic, electron spin resonance spectra, magnetic susceptibility measurement, molar conductance and thermal studies. The IR spectral data suggest that the ligand behaves as a dibasic bidentate with ON donor sequence towards metal ion. The molar conductivity data show them to be non-electrolytes. From the electronic, magnetic and ESR spectral data suggest that all the oxovanadium (IV) complexes have distorted octahedral geometry.

Crown Copyright © 2009 Published by Elsevier B.V. All rights reserved.

1. Introduction

Transition metal complexes of vanadium with Schiff bases have been amongst the most widely studied coordination compounds in the past few years, since they are found to be of importance are biochemical, analytical and antimicrobial agent [1,2], vanadium as an essential trace element found in the living organisms [3], discovery of enzymatic and physiological activities [4,5]. Schiff base and related vanadium complexes have important applications in biology and medicine [6] as well as in the catalysis associated with chemical and petrochemical processes [7], also act as inhibitors of enzymes [8] and antifungal/antibacterial agents [9]. Vanadates and oxovanadium (IV) species have shown great utility as tools in molecular biology for recognizing and understanding the binding sites and structure of proteins [2,10]. Schiff base of vanadium complexes is interesting, especially due to their pharmacological properties. The structurally documented bis(maltolato)oxovanadium (IV) has been found to be effective to regular glucose level in the plasma in diabetic rats with no significant effects on kidney functions [11,12]. Vanadium is commercially important in the conversion of crude oils into the transportation fuels [13]. In the present article we report pyrazolone derivative 1-phenyl-3-methyl-4-acyl(acyl = 4-carboxyaldehyde)-5-pyrazolone, their Schiff base ligands and their mononuclear Schiff base complexes of VO(IV).

2. Experimental

2.1. Materials

Analytical grade $VOSO_4{\cdot}5H_2O$ was used. 1-Phenyl-3-methyl-5-pyrazolone and their chloro and sulphoamido derivative (E-Merk), ethanol amine (BDH), 3-amino 1-propanol (Alfa-Alser) were used.

2.2. Instruments

Elemental analyses (C, H, N) were performed at RSIC, Lucknow. The vanadium metal was estimated by gravimetrically as vanadiumpentoxide (V_2O_5) after decomposing the complexes in concentrated sulphuric acid and nitric acid, igniting at 600 °C [14]. The conductance measurement of these complexes was carried out on the systronics direct reading conductivity meter type CM-82T. Infrared spectra were recorded with a Perkin Elmer IR spectrophotometer (4000–200 cm^{-1}) using KBr pellets. ^{1}H NMR spectra of the compounds were recorded with BRUKER AVANCE II 400 using $CDCl_3$ for ligands and Schiff base ligands and for metal complexes DMSO-d_6 as a solvent using TMS as an internal reference, at SAIF, Punjab University, Chandigarh. The ultraviolet and visible spectra of complexes in the 200–800 nm range were obtained in DMSO as a solvent, on a "SHIMADZU" UV 160A using quartz cell of 1 cm^3 opti-

---

* Corresponding author. Tel.: +91 261 2267957; fax: +91 261 2227312.
E-mail address: btthaker1@yahoo.co.in (B.T. Thaker).

1386-1425/$ – see front matter. Crown Copyright © 2009 Published by Elsevier B.V. All rights reserved.
doi:10.1016/j.saa.2009.08.041

cal path. The mass spectra of all VO(IV) complexes were recorded by Electro impact mass spectrometer, recorded at Department of Chemistry, Saurashtra University, Rajkot. The magnetic measurement of metal complexes at room temperature was carried out on Gouy balance as per the method suggested by Prasad et al. [15]. ESR spectra of all VO(IV) complexes were recorded by ESR Laboratory, SAIF, IIT, Bombay at RT and LNT for polycrystalline and solution state. TGA/DTA of the complexes were performed on a METTER M-3 thermo balance with microprocessor TA-3000 at a heating rate 10 °C/min at S.P. University, Vallabh Vidyanagar. The sample sizes are ranged in mass from 4.5 to 10 mg. The DSC of the complexes were performed on a METTER M-3 thermo balance with microprocessor TA-3000 at a heating rate 10 °C/min at Mantra, Surat.

2.3. Synthesis of ligands: (I), (II) and (III)

The ligands (I), (II) and (III) were prepared by condensation of 1-(2-chloro)-phenyl-3-methyl-5-pyrazolone (10.4 g, 0.05 mol), 1-(3-chloro)-phenyl-3-methyl-5-pyrazolone (10.4 g, 0.05 mol) and 1-(3-sulphoamido)-1-phenyl-3-methyl-5-pyrazolone (12.6 g, 0.05 mol) dissolved in DMF (10 ml, 0.05 mol), then cooled to 0 °C in an ice bath. The phosphoryl chloride (5.5 ml, 0.06 mol) was added drop wise at a rate to maintain the temperature between 10 and 20 °C. After the addition was completed, the reaction mixture was heated for 2.5 h for (I) and 3.5–4 h for (II) and (III) ligands, then poured into 1 l ice water in beaker. The resulting mixture was allowed to stand overnight; it was collected by filtration, washed with water, and dried. Crystallization was done with ethanol.

2.4. Synthesis of Schiff base ligands

The Schiff bases HL^1–HL^3 and HL^4–HL^6 were synthesized by refluxing methanolic solution of ligands I (2.33 g, 0.01 mol), II (2.33 g, 0.01 mol) and III (2.82 g, 0.01 mol) with ethanol amine (0.6 ml, 0.01 mol) and 3-amino-1-propanol (0.78 ml, 0.01 mol), respectively was heated at 60–70 °C in water bath for 4 h. The dark colored liquid was allowed to cool overnight. The solid thus obtained was filtered and washed with ether. Crystallization was done with ethanol and dried.

2.5. Synthesis of oxovanadium complexes

All the oxovanadium (IV) Schiff base complexes were prepared by 1:2 mole proportion of metal:ligand. The salt $VOSO_4 \cdot 5H_2O$ (2.53 g, 0.02 mol) was dissolved in water (15 ml) and the solution was added to a warmed (~65 °C) stirred (80 ml) methanolic solution of the corresponding Schiff bases ligands HL^1–HL^2 (5.59 g, 0.02 mol), HL^3 (6.16 g, 0.02 mol), HL^4–HL^5 (5.87 g, 0.02 mol) and HL^6 (6.12 g, 0.02 mol). After addition was over, 2 g of sodiumperchlorate (pH-6–7) was added to the solution and the reaction mixture was refluxed for 4–5 h and then concentrated to half of its volume. The resulting precipitates were filtered, washed successively with water and ethanol and dried.

3. Result and discussion

The elemental analyses, FT-IR and ^1H NMR spectral data are given in (Table 1a) for ligands I–III and in (Table 1b) for their Schiff base compounds HL^1–HL^6. The physical data of metal Schiff base complexes of VO(IV) have been given in (Table 2). There are in good agreements with the proposed stoichiometry.

3.1. Molar conductance

The molar conductance (Table 2) of the oxovanadium (IV) complexes in 10^{-3} M in DMSO as solvent observed in the range

Table 1a
Analytical, physical and spectral data of ligands.

Ligands	Color	Yield (%)	Melting point (°C)	Elemental analysis found % (calculated %)			Functional group IR frequencies (cm^{-1})		Functional group and chemical shifts δ in ppm		
				C	H	N	υ(C=O) cyclic	υ(C=O) aldehydic	—CH_3 proton	Phenyl multiplets proton	Aldehyde proton
I	Yellow	62.32	128	55.80(55.82)	3.70(3.83)	11.50(11.83)	1658	1628	2.20	7.26–7.42	9.75
II	Yellow	76.70	76	55.50(55.82)	3.70(3.83)	11.80(11.83)	1659	1627	2.13	7.25–7.40	9.74
III	Yellow	75.01	243	46.94(46.84)	3.90(3.94)	14.56(14.94)	1672	1628	2.14	7.43–7.63	9.45

Table 1b
Analytical, physical and spectral data of Schiff base ligands.

Schiff base ligands	Color	Yield (%)	Melting point (°C)	Elemental analysis found % (calculated %)			Functional group IR frequencies (cm^{-1})			Functional group and chemical shifts δ in ppm			
				C	H	N	υ(C=O) cyclic	υ(C=N) azomethine	—OH alkane	—CH_3 proton	–OH alkane	Phenyl multiplets proton	—CH=N proton
HL^1	Orange	71.73	161	55.50(55.82)	5.06(5.04)	15.09(15.02)	1658	1603	3313	2.21	5.37	7.08–7.87	8.03
HL^2	Light orange	75.74	115	55.50(55.82)	5.06(5.04)	15.09(15.02)	1659	1602	3361	2.17	5.40	7.07–7.86	8.02
HL^3	Pink	71.98	98	48.18(48.13)	4.98(4.97)	17.04(17.02)	1672	1601	3375	2.15	5.44	7.43–8.13	8.63
HL^4	Reddish brown	72.60	144	57.25(57.24)	5.53(5.49)	14.05(14.03)	1656	1603	3312	2.20	5.37	7.06–7.87	7.90
HL^5	Orange brown	73.12	117	57.25(57.24)	5.53(5.49)	14.05(14.03)	1661	1602	3369	2.18	5.34	7.07–7.88	7.91
HL^6	Reddish Brown	75.17	200	49.70(49.69)	5.40(5.36)	16.60(16.55)	1673	1601	3372	2.14	5.44	7.44–8.15	8.64

of 21–37 $ohm^{-1}\,cm^2\,mol^{-1}$, indicating non-electrolytic nature of these compounds and there is no counter ion present outside the coordination sphere of oxovanadium complexes [16,17].

3.2. FT-IR and ^1H NMR spectra of Schiff base ligands

The FT-IR spectra of the Schiff bases HL^1–HL^6 exhibit a medium band due to υ(OH) at 3375–3312 cm^{-1} due to —OH group of ethanol or propanol amine. Phenyl substituted at 4th position by —SO_2NH_2 group in pyrazoline compound, there is a sharp but less intense band observed at 3274 cm^{-1} in ligand (III), Schiff base HL^3 and HL^6 compounds. It indicates that this band is unaffected by Schiff base formation. The band due to υ(N—H) is also expected to appear around 3300–3200 cm^{-1} due to tautomerism of ligand, this band has not appeared [18,19]. Band appeared in the range of ~2916–2860 cm^{-1} is due to υ(C—H) of —CH_3 or —CH_2 groups. In Schiff base ligands the appearance of a strong band at 1673–1656 cm^{-1} is due to υ(C=O) of pyrazoline moiety, which remain unaffected on Schiff base formation. The band observed in 4-carbaldehyde due to υ(H—C=O) at 1628–1627 cm^{-1} in ligands, which has been disappeared and new band observed at 1605–1601 cm^{-1} due to υ(C=N) at 4th position on Schiff base formation by ethanol or propanol amine. Since, single crystal study of this compound shows that Schiff base molecule in solid state is in kito-immine form [20] as shown in Fig. 1.

^1H NMR spectra of Schiff base ligands HL^1–HL^6 show the high intensity signal appeared at δ 2.14–2.21 ppm having singlet multiplicity is due to —CH_3 group of pyrazoline ring at 3rd position. The free —OH proton of alkanol amine gives medium intense singlet at $\delta \sim 5.4$ ppm. The multiplate signals having different multiplicities observed in the range of δ 7.0–8.2 ppm is due to phenyl multiplate of which is substituted at 1st position of pyrazoline ring. The less intense singlet observed near δ 7.90–8.64 ppm is due to aldehydic C—H proton. There is one more signal having quintate degeneracy at δ 3.4–3.5 ppm, it may be due to middle —CH_2— proton of propanol [C=N—CH_2—CH_2—CH_2—OH] group. In the present ^1H NMR spectra of Schiff base compounds, the keto-enol tautomerism is so fast in solution state that is why 4-C—H or 5-OH proto could not be detected in ^1H NMR spectra.

3.3. FT-IR spectra of Schiff base complexes of oxovanadium (IV).

IR spectra of VO(IV) complexes (Table 3), the broad band centered at 3370–3337 cm^{-1} due to υ(O—H) of coordinated water molecule as well as —OH of the ethanol or propanol amine and remain undissociated after complex formation. In phenyl substituted SO_2NH_2 at 4th position Schiff base VO(IV) complexes show band at 3274 cm^{-1}, due to υ(N—H) of SO_2NH_2 group, which also remain unaffected on coordination. In the free Schiff base ligand the band appeared at ~1658–1674 cm^{-1} is assigned to υ(C=O) of pyrazoline ring at 5th position but the appearance of new band in the range of 1351–1346 cm^{-1} due to υ(C—O), is indicating complex formation take place by ketonic oxygen (after enolyzation) to the metal ion. On complex formation —C=CH—NH— kito-imine form converted to =C—CH=N— azomethine and new band observed at 1626–1619 cm^{-1} due to azomethine —C=N— group which is coordinated to metal ion [19]. All Schiff base VO(IV) compounds show medium band 970–995 cm^{-1}, is indicative of the υ(V=O) grouping in all the complexes [21]. The FT-IR spectra of VO(IV) complexes show new bands in the region 490–470 cm^{-1} and ~425 cm^{-1} which may be due to the formation M—O and M—N bands, respectively [22].

Table 2
Elemental analyses and some physical data of oxovanadium (IV) complexes.

Complexes	Color	Yield (%)	Melting point (°C)	Elemental analysis found % (calculated %)				Molar conductivity (ohm^{-1} cm^2 mol^{-1})	u_{eff} (B.M.)
				C	H	N	M		
$[VO(L^1)_2H_2O]$	Green	62.92	>250	47.63(48.61)	4.40(4.39)	12.97(13.08)	7.87(7.93)	21.00	1.76
$[VO(L^2)_2H_2O]$	Green	73.65	>250	47.65(48.61)	4.38(4.39)	12.93(13.08)	7.97(7.93)	32.45	1.76
$[VO(L^3)_2H_2O]$	Yellowish green	80.26	>250	42.75(42.71)	4.43(4.41)	15.30(15.32)	6.99(6.96)	36.78	1.73
$[VO(L^4)_2H_2O]$	Green	53.66	>250	50.19(50.16)	4.88(4.81)	12.61(12.53)	7.52(7.59)	23.80	1.77
$[VO(L^5)_2H_2O]$	Green	67.29	>250	50.20(50.16)	4.90(4.81)	12.46(12.53)	7.52(7.59)	32.45	1.74
$[VO(L^6)_2H_2O]$	Yellowish green	76.63	>250	44.23(44.26)	4.75(4.77)	14.70(14.74)	6.67(6.70)	35.70	1.73

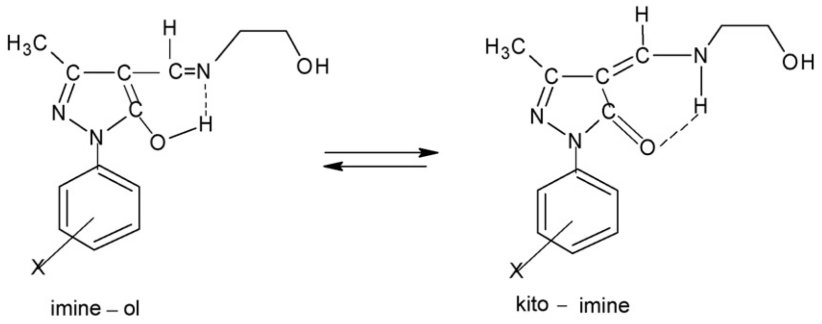

Fig. 1. Kito-imine tautomerism of Schiff base ligands in solid state.

Table 3
Infrared and ^{1}H NMR spectral data of oxovanadium (IV) complexes.

Complexes	Functional group and IR frequencies (cm^{-1})				Functional group and chemical shifts δ in ppm			
	υ(—OH) (broad band)	υ(C═N) coord.	υ(C—O) coord.	υ(V═O)	Methyl proton Singlet	—CH$_2$O alkane and ═N—CH$_2$	—OH alkane	Phenyl proton multiplets
$[VO(L^1)_2H_2O]$	3370	1619	1346	972	2.19	2.20–2.55	5.33	7.10–7.52
$[VO(L^2)_2H_2O]$	3373	1622	1343	976	2.53	2.57–3.18	5.41	7.16–7.40
$[VO(L^3)_2H_2O]$	3337	1625	1340	982	2.30	2.57–3.18	5.44	7.43–7.63
$[VO(L^4)_2H_2O]$	3350	1626	1357	991	2.22	2.40–3.25	5.39	7.10–7.52
$[VO(L^5)_2H_2O]$	3348	1620	1341	986	2.55	2.20–2.53	5.42	7.16–7.40
$[VO(L^6)_2H_2O]$	3340	1625	1350	989	2.40	2.58–3.18	5.43	7.43–7.63

3.4. ^{1}H NMR spectra of Schiff base complexes of oxovanadium (IV)

In ^{1}H NMR spectra of VO(IV) complexes (Table 3), the signal observed in complex molecules at δ 5.44–5.33 ppm with HL^1–HL^6 ligands attributed to —OH proton of the ethanol or propanol amine. This signal less resonate at same field in free Schiff base ligands and in complex molecules indicating nonparticipation of this —OH group. One more signal observed near down field region at δ 9.97–9.94 ppm due to water molecule proton, indicating presence of H_2O molecule in the complexes. These results can be substantiated by TGA studies.

3.5. Mass spectra

The mass spectrum of $[VO(L^1)_2H_2O]$ (Fig. 2) gives isotropic peak of *m*/*z* at 642,643 [M$^+$,(M+1)$^+$] which is corresponding to the composition $[VO(L^1)_2H_2O]$ (molecular mass = 642). This indicates that the Schiff base complex of VO(IV) is a mononuclear.

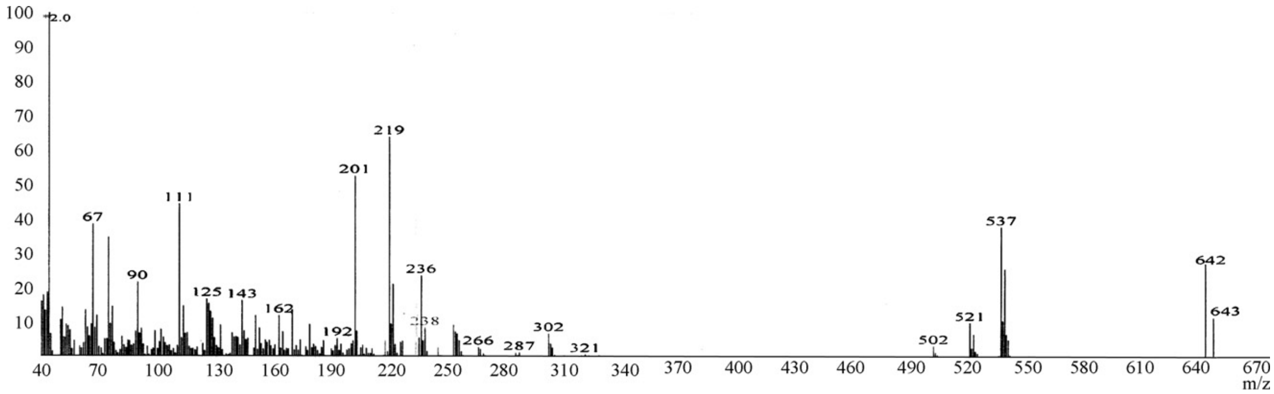

Fig. 2. Mass spectra of $[VO(L^1)_2H_2O]$.

Table 4
Electronic spectral data of oxovanadium (IV) complexes.

Complexes	d–d transition (cm^{-1})			Charge transfer band (cm^{-1})		
	$d_{xy} \rightarrow d_{xy,d_{yz}}$ (υ_1)	$d_{xy} \rightarrow d_{x^2-y^2}$ (υ_2)	$d_{xy} \rightarrow d_{z^2}$ (υ_3)			
$[VO(L^1)_2H_2O]$	13,227	16,638	22,675	28,653	32,573	33,333
$[VO(L^2)_2H_2O]$	13,440	17,006	25,641	27,700	29,498	36,101
$[VO(L^3)_2H_2O]$	13,458	17,421	23,809	26,246	28,490	33,670
$[VO(L^4)_2H_2O]$	13,210	17,331	24,096	28,490	32,467	36,630
$[VO(L^5)_2H_2O]$	13,440	17,006	25,641	27,777	29,497	36,496
$[VO(L^6)_2H_2O]$	13,422	17,421	23,752	26,246	28,490	37,313

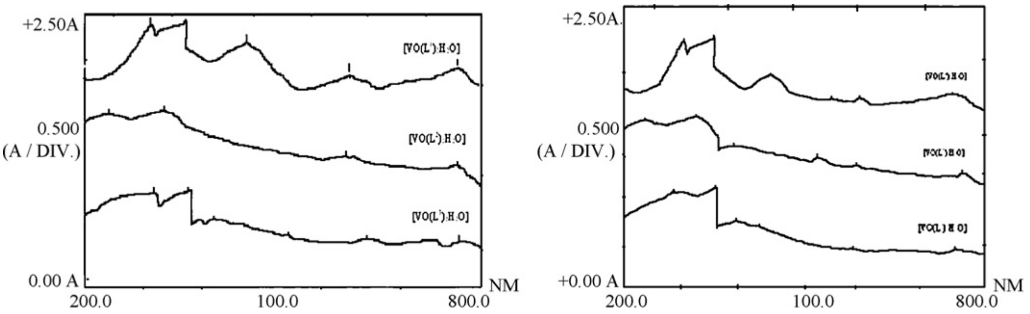

Fig. 3. Electronic spectra of $[VO(L^{1-6})_2H_2O]$.

3.6. Electronic spectra and magnetic moment

The electronic spectra of Schiff base complexes of oxovanadium (IV) in solution state recorded in DMSO as solvent shown in Fig. 3 and their relevant data are reported in Table 4. The electronic spectra of six oxovanadium (IV) complexes show intense band centered at 33,333–28,653 cm^{-1}, 36,101–27,700 cm^{-1} and 37,313–26,246 cm^{-1}, respectively, are due to charge transfer and inter-ligand ($\pi \rightarrow \pi^*$) transitions [23,24]. In the visible region, the solution electronic spectra of VO(IV) Schiff base complexes exhibit three d–d bands in the region 25,640–13,210 cm^{-1}. These bands may be assigned to the $\upsilon_1 \rightarrow {}^2B_{2g} \rightarrow {}^2E_g$, $\upsilon_2 \rightarrow {}^2B_{2g} \rightarrow {}^2B_{1g}$, $\upsilon_3 \rightarrow {}^2B_{2g} \rightarrow {}^2A_{1g}$ transitions. The observed magnetic moment (μ_{eff}) values (Table 2) is in the range of 1.73–1.76 B.M., indicating the VO(IV) Schiff base complexes are normal paramagnetic having one unpaired electron $s = 1/2$. There is no reduced magnetic moment, ruling out any antiferromagnetic interaction present in the molecules [25]. Therefore, VO(IV) Schiff base complexes are mononuclear. Theses two properties indicates the stereochemistry of VO(IV) Schiff base complexes may be distorted octahedral.

3.7. Electron spin resonance spectra

The ESR spectra of $[VO(L^1)_2H_2O]$ at RT and LNT are shown in Fig. 4. They show eight line spectra in both the temperature, indicating unpaired electron only coupled with mother nucleus having $I = 7/2$. The RT and LNT spectra of $[VO(L^1)_2H_2O]$ in solution state are shown in Fig. 5.

The ESR spectral data of $[VO(L^{1-3})_2H_2O]$ complexes are presented in Tables 5 and 6. The RT spectrum is a typical eight line pattern which shows that single vanadium is present in the molecules *i.e.* it is a monomer. In the frozen solution state, the spectrum shows two types of resonance components, one set due to parallel feature and the other set due to perpendicular feature, which indicates axially symmetric anisotropy with well resolved 16-line hyperfine splitting, characteristic of interaction between the electron and vanadium nuclear spins. The $g_{||}$ and $g_{\perp}$ values were computed from the spectra using DPPH free radical as g marker. The observed $g_{||}, g_{\perp}, |g|, A_{||}, A_{\perp}$, and $|A|$ values are well in accordance with the complexes indicate that the unpaired electron localized in d_{xy}

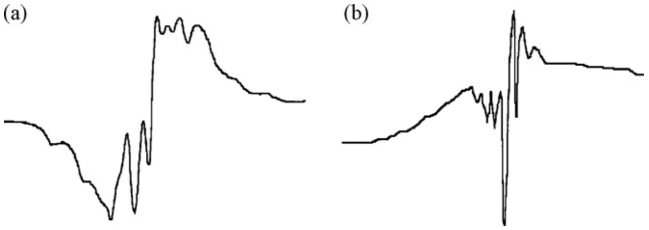

Fig. 4. The powder ESR spectra of $[VO(L^1)_2H_2O]$ complex at (a) RT and (b) LNT.

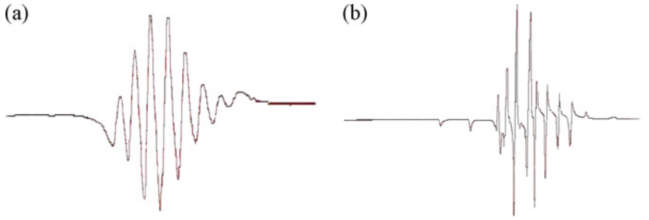

Fig. 5. The solution ESR spectra of $[VO(L^1)_2H_2O]$ complex at (a) RT and (b) LNT.

Table 5
g and A values of the powder ESR spectra of VO(IV) complexes at RT and LNT.

Complexes	RT						LNT					
	$g_{\|\|}$	$g_{\perp}$	$\|g\|$	$A_{\|\|}$ ($\times 10^{-4}$ cm^{-1})	$A_{\perp}$ ($\times 10^{-4}$ cm^{-1})	$\|A\|$ ($\times 10^{-4}$ cm^{-1})	$g_{\|\|}$	$g_{\perp}$	$\|g\|$	$A_{\|\|}$ ($\times 10^{-4}$ cm^{-1})	$A_{\perp}$ ($\times 10^{-4}$ cm^{-1})	$\|A\|$ ($\times 10^{-4}$ cm^{-1})
$[VO(L^1)_2H_2O]$	1.92	1.97	1.95	151.85	67.29	95.20	1.92	1.96	1.95	159.13	63.20	95.58
$[VO(L^2)_2H_2O]$	1.93	1.97	1.95	150.75	67.29	95.11	1.92	1.96	1.95	159.20	63.80	95.45
$[VO(L^3)_2H_2O]$	1.92	1.98	1.96	161.15	75.50	96.22	1.93	1.98	1.96	162.47	67.80	96.35

Table 6
g and A value of the solution* ESR spectra of VO(IV) complexes.

Complexes	$g_{\parallel}$	$g_{\perp}$	$\lvert g \rvert$	$A_{\parallel}$ ($\times 10^{-4}$ cm^{-1})	$A_{\perp}$ ($\times 10^{-4}$ cm^{-1})	$\lvert A \rvert$ ($\times 10^{-4}$ cm^{-1})
$[VO(L^1)_2H_2O]$	1.93	1.97	1.96	157.94	75.23	102.80
$[VO(L^2)_2H_2O]$	1.93	1.97	1.96	157.89	75.33	102.85
$[VO(L^3)_2H_2O]$	1.92	1.99	1.97	158.74	77.83	104.80

(* 70% DMF + 30% pyridine).
$\lvert g \rvert = 1/3(g_{\parallel} + 2g_{\perp})$.
$\lvert A \rvert = 1/3(A_{\parallel} + 2A_{\perp})$.

orbital of a molecule which exists in distorted octahedral geometry [26–28]. The molecular orbital coefficient α^2 or $(\beta_2{}^*)^2$ (covalent in-plane σ-bonding) and β^2 or $(\beta_1{}^*)^2$ (covalent in-plane π-bonding) were calculated by use the solution ESR spectral data and values are given in Table 7.

The value of the in-plane σ-bonding coefficient $(\beta_2{}^*)^2$ generally follows the σ donor strength of the ligand, *i.e.* $(\beta_2{}^*)^2$ decrease as covalent bonding increase. This parameter shows larger variation in present VO(IV) Schiff base complexes. The dependences of K on $(\beta_2{}^*)^2$ arise from participation of the empty 4*s* orbitals on the metal in σ-bonding to the ligands. The empty 4*s* orbital of the metal can overlap with the filled σ-levels of the basal ligands as effectively as can the $d_{x^2-y^2}$ orbital of the metal. The molecular orbital formed from the 4*s* orbital should put partial 4*s* density in a filled bonding orbital which in turn should undergo spin polarization by the d_{xy} electron. The extent of the ligand to metal interaction should be related to both energy of antibonding $d_{x^2-y^2}$ energy level and its orbital coefficient. The 4*s* contribution to K should proportional to the metal electron density in the filled orbital that contains contribution of 4*s* orbital. The delocalization in the σ-system of the complex is expressed by the bonding coefficient for the $d_{x^2-y^2}$ level.

The origin of the isotropic constant term K which is related to the amount of unpaired electron density on the vanadium nucleus has been subject of discussion. Since the orbital that contains the unpaired electron, d_{xy}, has zero electron density at the vanadium nucleus and does not mix with the metal 4*s* orbital (in C_{4V} symmetry), there is no direct way of putting unpaired electron density on the nucleus. The nonzero value of K must then arise from an indirect mechanism. Mc Gravey [29] suggests that variation can be explained by involving a spin polarization mechanism. The unpaired electron in the d_{xy} orbital formally creates unpaired electron density in filled 2*s* and 3*s* orbitals of the vanadium. In the absence of covalent bonding and 4*s* mixing, spin polarization should remain constant for all vanadium complexes and be equal to the free ion value, K_O. Taking into account covalent bonding, K shows depend on the d-orbital population for the unpaired electron, $K \sim (\beta_2{}^*)^2 K_O$.

An analysis of the bonding coefficients in the three complexes reveals that the strength of the equatorial plane π-bonding $(\beta_1{}^*)^2$ increases in the order 1.29 for $[VO(L^1)_2H_2O] < 1.32$ for $[VO(L^2)_2H_2O] < 1.63$ for $[VO(L^3)_2H_2O]$ and the equatorial in-plane σ bond $(\beta_2{}^*)^2$ strength stays about the same [31]. The $(e\pi^*)^2$, the bonding coefficient for d_{XZ} and d_{YZ} orbitals, measures the covalency of the oxovanadium bonds. It also indirectly shows the strength of in-plane ligands, since the stronger the in-plane donor atom, the less covalent is the oxovanadium bond.

Table 7
Bonding parameter of VO(IV) complexes.

Complexes	$(\beta_2{}^*)^2$	$(\beta_1{}^*)^2$	$(e\pi^*)^2$	K
$[VO(L^1)_2H_2O]$	0.683	<1	0.974	0.760
$[VO(L^2)_2H_2O]$	0.681	<1	0.967	0.760
$[VO(L^3)_2H_2O]$	0.645	<1	0.976	0.786

G value calculated by using the following equations:

$$G = \frac{g_{\parallel} - 2.002}{g_{\perp} - 2.002}$$

If $G < 4.0$, the ligand forming the complex is regarded as a strong field ligand. The G value of the complexes $[VO(HL^1)_2H_2O]$, $[VO(HL^2)_2H_2O]$ and $[VO(HL^3)_2H_2O]$ at room temperature are 3.83, 3.83 and 3.47 and at LNT are 2.42, 2.42 and 3.27, respectively, indicating that the Schiff base ligands are strong field ligands and the metal–ligand bonding in these complexes is covalent.

The bonding parameters were calculated by using the following equations [30,31]:

$$(A_{\parallel} - A_{\perp}) = 6/7(\beta_2{}^*)^2 P - (g_e - g_{\parallel})P + 5/14(g_e - g_{\perp})P$$

$$g_e - g_{\parallel} = \frac{8(\beta_1{}^*)^2(\beta_2{}^*)^2\xi}{\Delta E_1 d_{xy} \rightarrow d_{x^2-y^2}}$$

$$g_e - g_{\perp} = \frac{2(\beta_2{}^*)^2(e\pi{}^*)^2\xi}{\Delta E_2 d_{xy} \rightarrow d_{xz,yz}}$$

$$\lvert A \rvert = -PK - (g_e - \lvert g \rvert)P$$

$g_e = 2.0023$, $A_{\parallel}$, $A_{\perp}$ and $\lvert A \rvert$ are taken to be negative [30], P is the free ion dipole term = 128×10^{-4} cm^{-1}, ξ = spin-orbit coupling constant = 170 cm^{-1}, ΔE_1 = electronic transition energy of $d_{xy} \rightarrow d_{x^2-y^2}$ ΔE_2 = electronic transition energy of $d_{xy} \rightarrow d_{xz,yz}$.

3.8. *Thermal study*

In the present studies of the metal complexes of VO(IV), we select non-isothermal mode for TGA, DTA and DSC techniques. From the TGA curves of complexes $[VO(L^1)_2H_2O]$ and $[VO(L^3)_2H_2O]$, they have been observed that there are four steps and $[VO(L^2)_2H_2O]$, $[VO(L^4)_2H_2O]$, $[VO(L^5)_2H_2O]$ and $[VO(L^6)_2H_2O]$, they have been observed two steps, in the decomposition of VO(IV) complexes. But from the DTA curves of the complexes, we found two endothermic peaks. In DSC curves of complexes are identical exhibit two endothermic peaks in the range of 120–180 °C and 305–430 °C corresponding to the detachment of coordinated H_2O molecule and pyrolysis of organic molecules [32], respectively, which are shown in Figs. 6 and 7. The first mass loss 3.25–4.00% (2.81–3.89% cala.) up to 180 °C is in good agreement with loss of one coordinated water molecule. At 600–700 °C, the stable metal oxide V_2O_5 was formed. The activation energy ΔE^*calculated by Broido graphical method and Broido plots are shown in Fig. 8. From the DSC curve, we found out the ΔH^* and ΔS^* and their values are given in Table 8.

3.8.1. *Broido's method*

A Broido has suggested a simple and sensitive graphical method for the treatment of TGA data. According to this method, the weight at any time t (wt.) is related to the fraction of initial molecules not

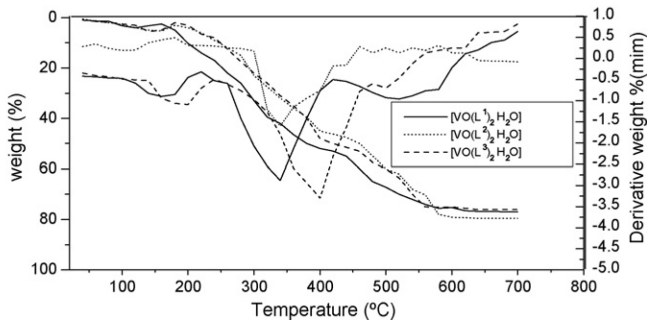

Fig. 6. Comparison of TGA/DTA curve of $[VO(L^{1-3})_2H_2O]$ complexes.

yet decomposed (y) by the equation:

$$Y = \frac{N}{N_0} = \frac{w_t - w_a}{w_0 - w_a} \tag{i}$$

where w_0 is the initial weight of the materials and w_a is the weight of residue at the end of decomposition.

For isolated pyrolysis:

$$\frac{dy}{dt} = -Ky^n \tag{ii}$$

If

$$K = Ae^{-E/RT} \tag{iii}$$

And if T is linear function of time t, therefore:

$$T = T_0 + \beta_t \tag{iv}$$

Then Eqs. (ii)–(iv) may be combined as under:

$$\frac{dy}{dn} = -\left(\frac{A}{\beta}\right) e^{E/RT} \cdot dt \tag{v}$$

where $\beta = dT/dt$, the heating rate.

Eq. (v) is integrated as:

$$\int_Y^1 \frac{dy}{dn} = \frac{A}{\beta} \int_{To}^{T} e^{-E/RT} \cdot dT \tag{vi}$$

For the first order kinetic ($n = 1$) which complex degradation usually:

$$\int_Y^1 \frac{dy}{y} = -\ln y = \ln\left(\frac{1}{y}\right) \tag{vii}$$

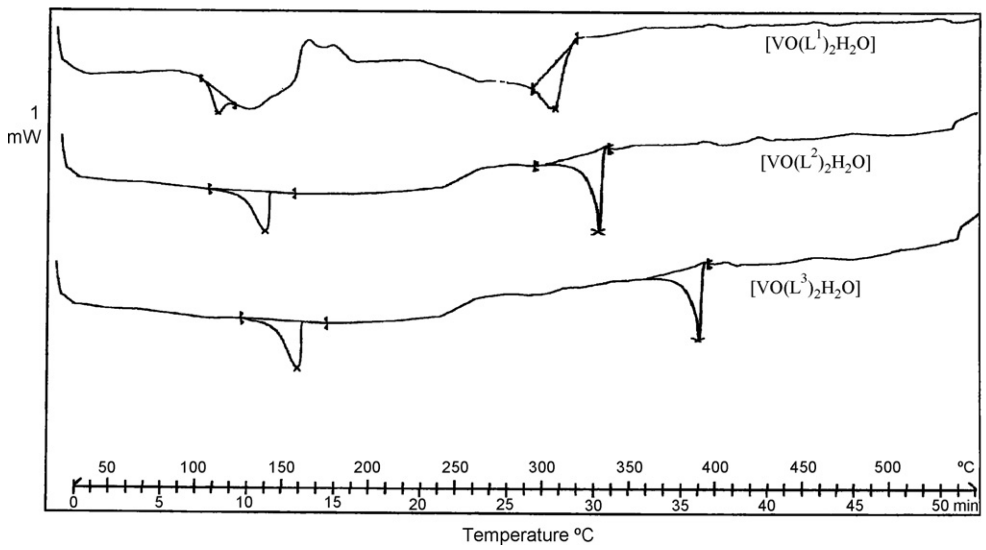

Fig. 7. DSC curve of $[VO(L^{1-3})_2H_2O]$ complexes.

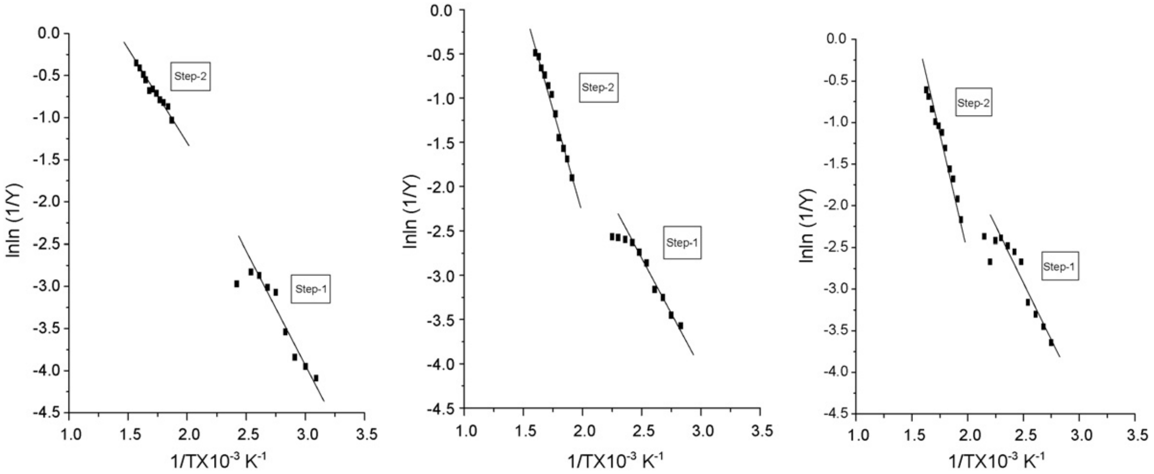

Fig. 8. Broido plots of $[VO(L^{1-3})_2H_2O]$ complexes.

Table 8
Thermal study of oxovanadium (IV) complexes.

Complexes	Step	Step analysis temperature °c		ΔE^* (K cal mol^{-1})	ΔH^* (K cal mol^{-1})	ΔS^* (K cal mol^{-1})
		Start	End			
$[VO(L^1)_2H_2O]$	I	100	160	13.15	78.90	0.23
	II	290	360	24.58	103.91	0.17
$[VO(L^2)_2H_2O]$	I	110	170	8.69	75.52	0.18
	II	280	380	17.84	102.84	0.16
$[VO(L^3)_2H_2O]$	I	130	170	6.94	80.22	0.19
	II	370	430	27.84	113.86	0.16
$[VO(L^4)_2H_2O]$	I	120	170	7.02	81.20	0.20
	II	150	430	23.85	101.22	0.14
$[VO(L^5)_2H_2O]$	I	100	170	8.50	77.78	0.17
	II	320	380	17.08	105.21	0.17
$[VO(L^6)_2H_2O]$	I	120	180	5.81	80.81	0.18
	II	280	380	23.49	115.95	0.18

On integrating and taking log of both sides of Eq. (vi) following equation obtained.

$$\ln\left[\ln\left(\frac{1}{y}\right)\right] = \left(\frac{E}{RT_{m+1}}\right)\ln T + \text{constant} \qquad \text{(viii)}$$

Thus, a plot of ln [ln(1/y)] vs. 1/T yields is straight line, whose slope is directly related to E_a:

$$-E_a = \text{slope} \times 2.303 \times R$$

where E_a is activation energy and R is the gas constant.

Application of this method used to determine the kinetic parameter for complexes.

The term of DSC was apparently first used by Waston et al. to describe the instrument technique developed by the PerkinElmer Corporation. The curve obtained is recording of heat flow dH/dt, in m cal/s, as a function of temperature. Thermodynamic sense, an endothermic curve peak is indicated by a peak in the upward direction (increase in enthalpy) while an exothermic peak is recorded in the opposition direction. In all appearances, the DSC curve looks very similar to that of a DTA curve except for the ordinate axis units. As in DTA the area enclosed by the DSC curve peak is directly proportional to the enthalpy change.

$$\text{area} \propto \Delta Hm$$

$$\text{area} = K\Delta Hm$$

Except that K is independence of temperature from the enthalpy, entropy changes are also calculated by using equation as below:

$$\Delta S = \frac{\Delta H}{T}$$

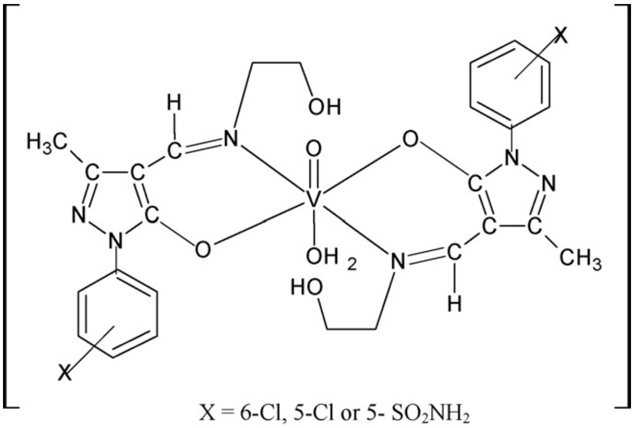

Fig. 9. General structures of Schiff base complexes of $[VO(L^{1-3})_2H_2O]$.

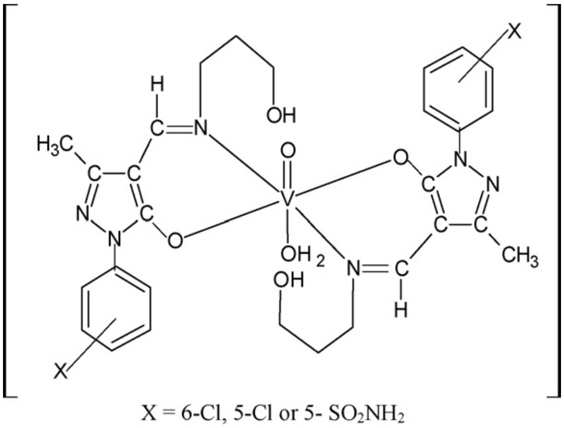

Fig. 10. General structures of Schiff base complexes of $[VO(L^{4-6})_2H_2O]$.

ΔS is the entropy change in K cal/mol K. T is the temperature in Kelvin.

4. Conclusion

The IR and ^{1}H NMR spectral data suggest that the Schiff base ligand behaves as a dibasic bidentate with ON donor sequence towards metal ion. The molar conductivity data show them to be non-electrolytes. Presence of one water molecule shown by TGA/DTA and DSC curve. Thermal stability of complexes 1 to 6 in the order 1 > 3 > 4 > 6 > 2 > 5 on the basis of activation energy parameter. From the magnetic, electronic and ESR spectral data suggest that all the oxovanadium (IV) complexes have distorted octahedral geometry shown in Figs. 9 and 10.

References

[1] M.R. Maurya, N. Bharti, A. Azam, Eur. J. Med. Chem. 35 (2000) 481.
[2] N.D. Chasteen, in: L.J. Berliner, J. Reuben (Eds.), “Biological Magnetic Resonance”, vol. 3, Plenum press, NY, 1981, 53, p. 119.
[3] D. Rehder, The bioinorganic chemistry of vanadium, Angew. Chem. Int. Ed. Engl. 30 (1991) 148–267.
[4] K.H. Thomson, J.H. McNeil, C. Orvig, Chem. Rev. 97 (1999) 2561.
[5] D.C. Crans, S.S. Amin, A.D. Keramidas, Chemistry of relevance to vanadium in the environment, in: J.O. Nriagu (Ed.), Vanadium in the Environment. Part 1. Chemistry and Biochemistry, Weiley, New York, 1998 (Chapter 4).
[6] K.M. Btichel, Pflanzenschiitz and Schiidlingbekiimpfung, G. Thieme Verlag, Stuttgart, 1977.
[7] W. Holzer, R.M. Claramunt, M.P. Torralba, D. Gaggi, T.H. Brechmer, Eur. J. Org. Chem. (2003) 1209.
[8] M. Hassan, Z.H. Chohan, A. Scozzafava, C.T. Suparan, Carbonic anhydrase inhibitors, “*Schiff base of aromatic and heterocyclic sulfominds and their metal complexes*”, J. Enz. Inhib. Med. Hem. 19 (2004) 263.
[9] Z.H. Chohan, C.T. Supuran, A. Scozzafava, Metal binding and antibacterial activity of ciprofloxacin complexes, J. Enz. Inhib. Med. Chem. 20 (2004) 303.

[10] De Boer, E. Boon, K. Wever, Biochemistry 27 (1988) 1629.

[11] (a) G. Tomlin (Ed.), "The Pesticide Manual", 10th ed., British Crop Protection Pub., Surrey, 1991;
(b) H. Takaishi, I. Nakao, H. Hamaguchi, Jpn. Kakai Tokkyo Koho JP. 06, 70, 015 (1994).(Chem. Abstr., 1994, 121,108779s).;
(c) B. Boehner, R.G. Hall, Ger. Of Jen. DE 4, 139, 849, (Chem. Abstr., 1992, 117, 131386n) (1992).

[12] G.B. Morin, Cell 59 (1989) 521.

[13] J.G. Speight, The Chemistry and Technology of Petroleum Chemical Industry, 30, Marcel Dekker, New York, 1983.

[14] R.N. Mohanti, V. Chakravortty, K.C. Dash, Ind. J. Chem. 30A (1991) 457.

[15] M. Prasad, S.S. Dharmati, S.V. Gokhale, Proc. Ind. Acad. Sci. 20A (1944) 224.

[16] W.J. Geary, The use of conductivity measurement in organic solvents for the characterization of coordination, Coord. Chem. Rev. 7 (1971) 81–122.

[17] A.S. Aswar, J.T. Makode, Ind. J. Chem. 43-A (2004) 2120.

[18] K. Nakamoto, Infrared and Raman Spetra of Inorganic and Coordination Compounds, III ed., John wiley and sons, New York, 1978, 242.

[19] R.C. Maurya, H. Singh, A. Pandey, Synth. React. Inorg. Met. Org. Chem. 32 (2) (2001) 231.

[20] B.T. Thaker, K.R. Surti, S. Oswal, R.N. Jadeja, V.K. Gupta, Struct. Chem. 18 (2007) 295–310.

[21] J. Selbin, T.R. Oetolano, F.J. Smith, Inorg. Chem. 2 (1963) 1315.

[22] K.R. Surti, B.T. Thaker, J. Coord. Chem. 59 (11) (2006) 1191.

[23] T. Ghoshh, C. Bandyopadhyay, Trans. Met. Chem. 30 (2005) 404.

[24] I. Sakryan, N. Gunduz, T. Gunduz, Synth. React. Inorg. Met. Org. Chem. 31 (7) (2001) 1175.

[25] G.R. Hausan, T.A. Kabanos, A.D. Keramidas, D.M. Entzatos, A. Terzis, Inorg. Chem. 31 (1992) 2587.

[26] W. Goedey, Theory and Application of Electronic Spin Resonance, John wiley, New York, 1980.

[27] S.K. Gupta, D. Raina, Trans. Met. Chem. 22 (1997) 327.

[28] A. Syamal, K.S. Kale, Ind. J. Chem. 17A (1979) 518.

[29] B.R. Mc Gravey, J. Chem. Phys. 41 (1964) 3743.

[30] B.T. Thaker, J. Lekhadia, A. patel, P. thaker, Trans. Met. Chem. 19 (1994) 623–631.

[31] E. Martell, Coordination Chemistry, vol. 1, Van Nostrand Reinhold Co., New York, 1971, p. 217.

[32] K. Dey, K. Chakraborty, Ind. J. Chem. 38A (1999) 381.